Large magnetoresistance tunnelling through a magnetically modulated nanostructure

2003 J. Phys.: Condens. Matter 15 1267

(http://iopscience.iop.org/0953-8984/15/8/311)

INSTITUTE OF PHYSICS PUBLISHING JOURNAL OF PHYSICS: CONDENSED MATTER

J. Phys.: Condens. Matter **15** (2003) 1267–1275 PII: S0953-8984(03)56293-2

Large magnetoresistance tunnelling through a magnetically modulated nanostructure

Mao-Wang Lu and Li-De Zhang

Institute of Solid State Physics, Chinese Academy of Sciences, PO Box 1129, Hefei 230031, People's Republic of China

Received 19 November 2002
Published 17 February 2003
Online at stacks.iop.org/JPhysCM/15/1267

Abstract

Based on a combination of an inhomogeneous magnetic field and a two-dimensional electron gas, we have constructed a giant magnetoresistance nanostructure, which can be realized experimentally by the deposition of two parallel ferromagnetic strips on top of a semiconductor heterostructure. We have theoretically studied the magnetoresistance for electrons tunnelling through this nanostructure. It is shown that there exists a significant transmission difference between the parallel and antiparallel magnetization configurations, which leads to a large magnetoresistance. It is also shown that the magnetoresistance ratio strongly depends not only on incident electronic energy but also on the ferromagnetic strips, and thus a much larger magnetoresistance ratio can be obtained by properly fabricating the ferromagnetic strips in the system.

1. Introduction

The discovery of the giant magnetoresistance (GMR) effect in 1988 [1] has attracted a great amount of experimental and theoretical attention to GMR systems in recent years [1–16]. At present, the GMR effect has given rise to many significant practical applications in magnetic information storage [2, 3], including ultrasensitive magnetic field sensors, read heads, random access memories and so on [4]. The GMR effect is usually observed in a sandwiched structure composed of two ferromagnetic layers separated by a thin nonmagnetic layer, when the relative orientations of the magnetizations of these two magnetic layers are switched by an externally applied magnetic field from an antiparallel (AP) to a parallel (P) alignment. In the P configuration, the conductance of the structure is higher since the spin-dependent scattering of the carriers is minimized, while the conductance is lower for the AP configuration due to the maximized spin-dependent carrier scattering. In the GMR device, the current can either be perpendicular to the planes of the layers (the so-called CPP geometry) or be parallel to the interfaces (the CIP geometry). Moreover, the degree of the GMR effect is usually characterized in the magnetoresistance ratio defined by $\mathrm{MR} = (G_P - G_{AP})/G_{AP}$, where G_P and G_{AP} are

0953-8984/03/081267+09$30.00

the conductances for P and AP alignments respectively. For a specific GMR device, one hopes from the viewpoint of practical applications that the system possesses high MR under a relatively low saturation magnetic field. High values of the MR up to 220% have been reported at low temperatures [5]. In addition, the CPP geometry generally has a higher MR than the CIP geometry, but experiments on the GMR effect are mostly performed with the latter geometry because the experimental set-up in CIP is easier to achieve than in CPP [6, 14, 16].

Very recently, using δ-function magnetic barriers on the two-dimensional electron gas (2DEG), a GMR device has been proposed and studied [6]. It has been found that although the average magnetic field of the structure is zero this kind of system possesses very high MR, and the GMR effect makes no use of the spin degree of freedom, distinct from the situation in conventional GMR devices. However, in [6] the use of an ideal magnetic profile can make the attained results deviate from practical cases. In addition, in order to differentiate GMR devices in the conventional sense one should call the kind of device defined by magnetic-barrier nanostructures GMR-like or large magnetoresistance (LMR) devices. In this paper, based on a combination of magnetic materials and semiconductor heterostructures, we have constructed a realistic LMR device to study the GMR-like effect in a magnetic-barrier nanostructure. In our work we employ the exact magnetic profiles instead of the ideal ones, and the effect of system parameters on the MR of the device is examined in detail.

2. Model and formulation

The system we consider in this work is schematically depicted in figure 1, which is based on a combination of non-homogeneous magnetic fields (magnetic barriers) and a 2DEG. This system can be experimentally realized [7, 8] by the deposition, on top of a semiconductor heterostructure, of two parallel metallic ferromagnetic strips with magnetizations parallel to the 2DEG lying in the xy-plane, where the parameters d, h and M_0 stand for the width, thickness and magnetization of the strip respectively, and z_0 is the distance between the strip and the 2DEG. Here, figures 1(a) and (b) correspond to the P and AP configurations respectively for the GMR-like device, which can be switched by means of an externally applied magnetic field. The magnetic field produced by the magnetized ferromagnetic strip in the 2DEG can be expressed by [9]

$$\begin{aligned} &\boldsymbol{B} = B_z(x)\hat{z}, \\ &B_z(x) = M_0 h\left\{\frac{z_0}{[(x+d/2)^2+z_0^2]} - \frac{z_0}{[(x-d/2)^2+z_0^2]}\right\}, \end{aligned} \tag{1}$$

while its vector potential can be given, in the Landau gauge, by

$$\begin{aligned} &\boldsymbol{A} = [0, A_y(x), 0], \\ &A_y(x) = M_0 h\left\{\tan^{-1}\left[\frac{(x+d/2)}{z_0}\right] - \tan^{-1}\left[\frac{(x-d/2)}{z_0}\right]\right\}. \end{aligned} \tag{2}$$

The Hamiltonian describing such a 2DEG system in the framework of the parabolic-band effective-mass approximation can be written as

$$H = \frac{p_x^2}{2m_e^*} + \frac{[p_y + eA_y(x)]^2}{2m_e^*}, \tag{3}$$

where m_e^* and (p_x, p_y) are the effective mass and the momentum of the tunnelling electron. Because the system is translationally invariant along the y direction, the solution of the stationary Schrödinger equation $H\Psi(x, y) = E\Psi(x, y)$ can be written as a product $\Psi(x, y) =$

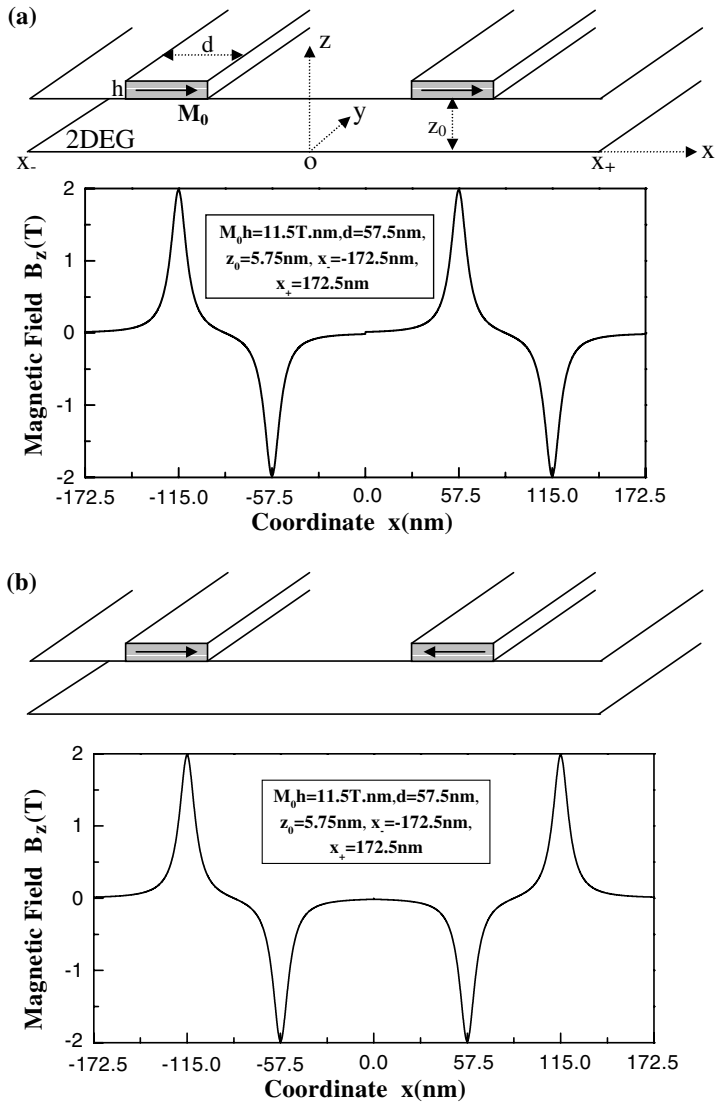

Figure 1. Schematic illustration of the GMR-like device, where the structural parameters are chosen to be $M_0h = 11.5$ T nm, $d = 57.5$ nm, $z_0 = 5.75$ nm, and the left and right ends of the nanostructure are located at $x_- = -172.5$ nm and $x_+ = 172.5$ nm. Figures 1(a) and (b) correspond to the P and AP alignments respectively.

$e^{iqy}\psi(x)$, where q is the y component of the wavevector of the electron. Furthermore, the wavefunction $\psi(x)$ satisfies the following one-dimensional (1D) Schrödinger equation:

$$\left\{\frac{d^2}{dx^2} - \left[q + \frac{e}{\hbar}A_y(x)\right]^2 + \frac{2m_e^*}{\hbar^2}E\right\}\psi(x) = 0. \tag{4}$$

For convenience, in what follows we introduce the effective potential of the above nanostructure

$$U_{eff}(x, q) = \frac{1}{2m_e^*}[\hbar q + eA_y(x)]^2. \tag{5}$$

Clearly, the effective potential of the nanostructure depends not only on the magnetic configuration $B_z(x)$ but also on the electron wavevector q, i.e. on the momentum parallel to the magnetic barrier. The q-dependence renders the motion of electrons an essentially two-dimensional (2D) process as would be expected from the classical analogy. From the dependence of the U_{eff} on the magnetic profile $B_z(x)$, one can easily see that for the device presented in figure 1, when the parallel alignment (figure 1(a)) turns to the inverse (figure 1(b)), U_{eff} varies substantially. Moreover, as discussed below, it is this variation of the effective potential induced by its dependence on the magnetic configuration that results in the LMR effect in the nanostructure involved, and the structural parameters of the system greatly influence the magnitude of its LMR.

For our considered nanostructure, since it has a realistic magnetic profile $B_z(x)$ and thus a complex effective potential U_{eff} in the structural region $[x_-, x_+]$, it is impossible to exactly solve the equation of motion (4). Therefore, we adopt the approximate method in [10]. Without any loss of generality, in both incident and outgoing regions of the nanostructure, the wavefunctions can be assumed as $\psi(x) = \mathrm{e}^{\mathrm{i}kx} + r\mathrm{e}^{-\mathrm{i}kx}$, $x < x_-$ and $t\mathrm{e}^{\mathrm{i}kx}$, $x > x_+$ respectively, where $k = \sqrt{2E - q^2}$, r is the reflection amplitude and t is transmission amplitude. By using transfer-matrix technology [11], we can obtain the transmission coefficient through the whole nanostructure

$$T(E, q) = |t|^2. \tag{6}$$

Once the $T(E, q)$ is known, the conductance of the nanostructure at zero temperature can be calculated in the ballistic regime as the average electron flow over half the Fermi surface from the well-known Landauer–Buttiker formula, and is given by

$$G(E_F) = G_0 \int_{-\pi/2}^{\pi/2} T(E_F, \sqrt{2E_F}\sin\theta)\cos\theta \,\mathrm{d}\theta, \tag{7}$$

with θ the incident angle relative to the x direction. The conductance is presented in units of $G_0 = 2e^2 m_e^* v_F L_y / h^2$, where v_F is the Fermi velocity and L_y is the longitudinal length of the nanostructure.

3. Results and discussion

First, to demonstrate the discrepancy of transmission for electrons tunnelling through the parallel configuration (figure 1(a)) and the AP one (figure 1(b)), we have calculated the corresponding transmission coefficients of T_P and T_{AP}. Figure 2 shows these transmission coefficients versus the incident energy E for electrons with different wavevector $q = 0.0\ \mu\mathrm{m}^{-1}$ (full curve), $8.7\ \mu\mathrm{m}^{-1}$ (dashed curve) and $-8.7\ \mu\mathrm{m}^{-1}$ (dotted curve), where figures 2(a) and (b) correspond to the P and AP configurations, respectively. The structural parameters are chosen to be $M_0 h = 11.5$ T nm, $d = 57.5$ nm and $z_0 = 5.75$ nm for both configurations. In our calculations the material is taken as the typical GaAs system, where $m_e^* = 0.067\ m_e$ with m_e being the free-electron mass, and the left and right ends of nanostructures are located at $x_- = -172.5$ nm and $x_+ = 172.5$ nm respectively. For the P configuration, the transmission spectrum exhibits clear longitudinal-wavevector-dependent tunnelling features as confirmed previously [9, 10], due to the essentially 2D process for electrons moving through the magnetic-barrier structures. Moreover, one can obviously see that in the low-energy region there are several resonant peaks with unity values. This can be expected because for the considered wavevectors q the effective potential U_{eff} has a symmetric multiple barrier structure for the P configuration, where the process of electron motion is resonantly tunnelling through these barriers. When the system switches from the P configuration to the AP configuration, one can

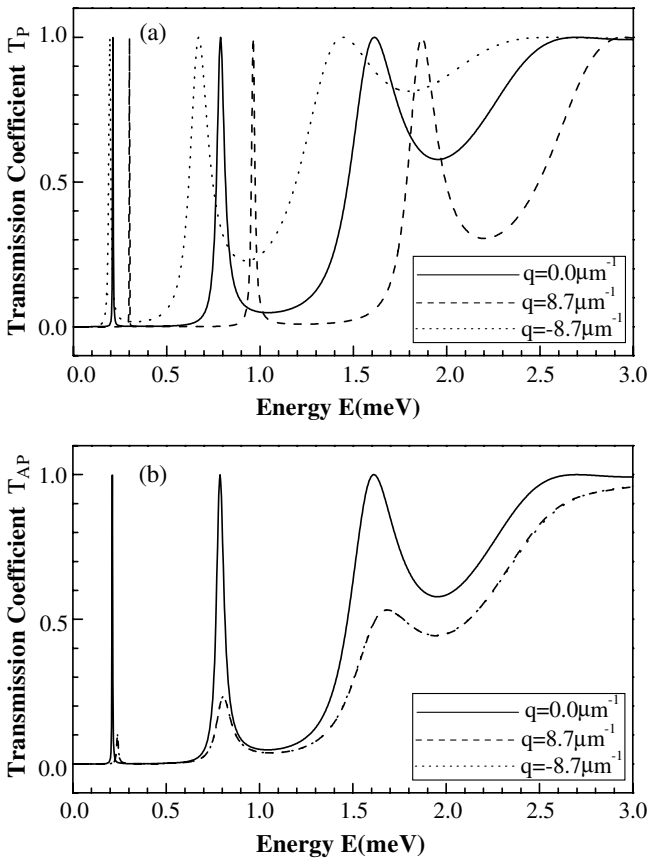

Figure 2. The transmission coefficients of electrons tunnelling through the P and AP configurations, respectively, where the structural parameters are the same as in figure 1 and the wavevector components of electron are taken to be $q = 0.0\ \mu\text{m}^{-1}$ (solid curve), $8.7\ \mu\text{m}^{-1}$ (dashed curve), and $-8.7\ \mu\text{m}^{-1}$ nm (dotted curve).

see from figure 2(b) that the electron transmission is greatly altered because of the variation of the U_{eff} induced by the structure. There are several prominent features in the transmission spectrum that we would like to summarize here.

(1) In the case of normal incidence (i.e. $q = 0$), the transmission coefficient for the AP alignment is exactly the same as that for the P alignment because their corresponding effective potentials are identical.
(2) The transmission coefficient of electrons with wavevector q is equal to that with $-q$, i.e. the dashed curve and dotted curve in figure 2(b) overlap each other. For the AP alignment, the magnetic profile $B_z(x)$ and the corresponding vector potential $A_y(x)$ are symmetric and antisymmetric respectively with respect to the x axis, which results in the effective potential $U_{eff}(x, q) = U_{eff}(x, -q)$ according to the well-known fact that for particles traversing a potential in opposite directions the transmission is always equal. Therefore, such a symmetry leads to the invariance of the transmission with respect to the replacement $q \to -q$, i.e. in figure 2(b) the dashed curve and dotted one are the same.
(3) When $q \neq 0$, the transmission coefficient is strongly suppressed for electrons tunnelling through the AP configuration. This is because for the AP alignment the effective

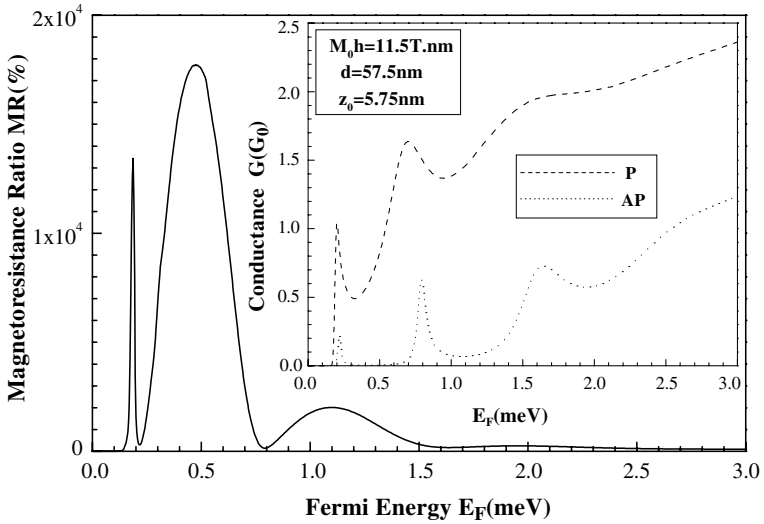

Figure 3. The magnetoresistance ratio MR as a function of the Fermi energy E_F for the system parameters which are the same as in figure 2. The inset gives the conductances G_A (dashed curve) and G_{AP} (dotted curve) of the P and AP alignments respectively, where the conductances are in units of $G_0 = 2e^2 m_e^* v_F L_y / h^2$.

potential U_{eff} is antisymmetric for electric multiple-barriers or wells, where the electron transmission is incomplete.

Since there exists an evident difference of transmission between the P and AP alignments, it is expected that the conductance of the P configuration will differ greatly from that of the AP structure. Indeed, our calculated results also confirm this discrepancy in the conductances G_P and G_{AP}. In the inset of figure 3 we present the conductances G_P (dashed curve) and G_{AP} (dotted curve) for the P and AP alignments versus the Fermi energy E_F, where the structural parameters are the same as in figure 2 and the conductance is in units of G_0. The strong suppression of the conductance G_{AP} is clearly seen due to the great reduction of the transmission coefficient T_{AP} in contrast to the P alignment. It is this large suppression of the conductance of the AP alignment that results in an evident GMR-like effect in the device. Figure 3 shows the magnetoresistance ratio MR as a function of the Fermi energy E_F for our considered nanostructure. It is obvious that the MR can be up to $10^4\%$ at certain Fermi energy and varies drastically with the Fermi energy E_F (namely, it exhibits evident oscillation with respect to the Fermi energy). It is also evident that the GMR-like effect mainly occurs in the low Fermi-energy region and the MR reduces to zero for large E_F.

Finally, we examine the effect of the ferromagnetic strip and its position relative to the 2DEG on the LMR for the system shown in figure 1. Figure 4(a) shows the MR versus the Fermi energy E_F for the system parameters ($M_0h = 11.5$ T nm, $d = 57.5$ nm, and $z_0 = 17.25$ nm), where the inset gives the conductances of the P (dashed curve) and AP (dotted curve) alignments. Comparing with the case of figure 3, one can see that both the G_P and the G_{AP} curves shift towards the low-energy region with increase of z_0, and the first conductance peak disappears. Furthermore, the corresponding MR curve also moves to the left and the oscillation peaks become much sharper. Figure 4(b) presents the GMR effect of the system, in which the structural parameters are the same as in figure 3 except for $d = 86.25$ nm and the inset also shows the conductance G_P and G_{AP}. From the inset one can see that for wider

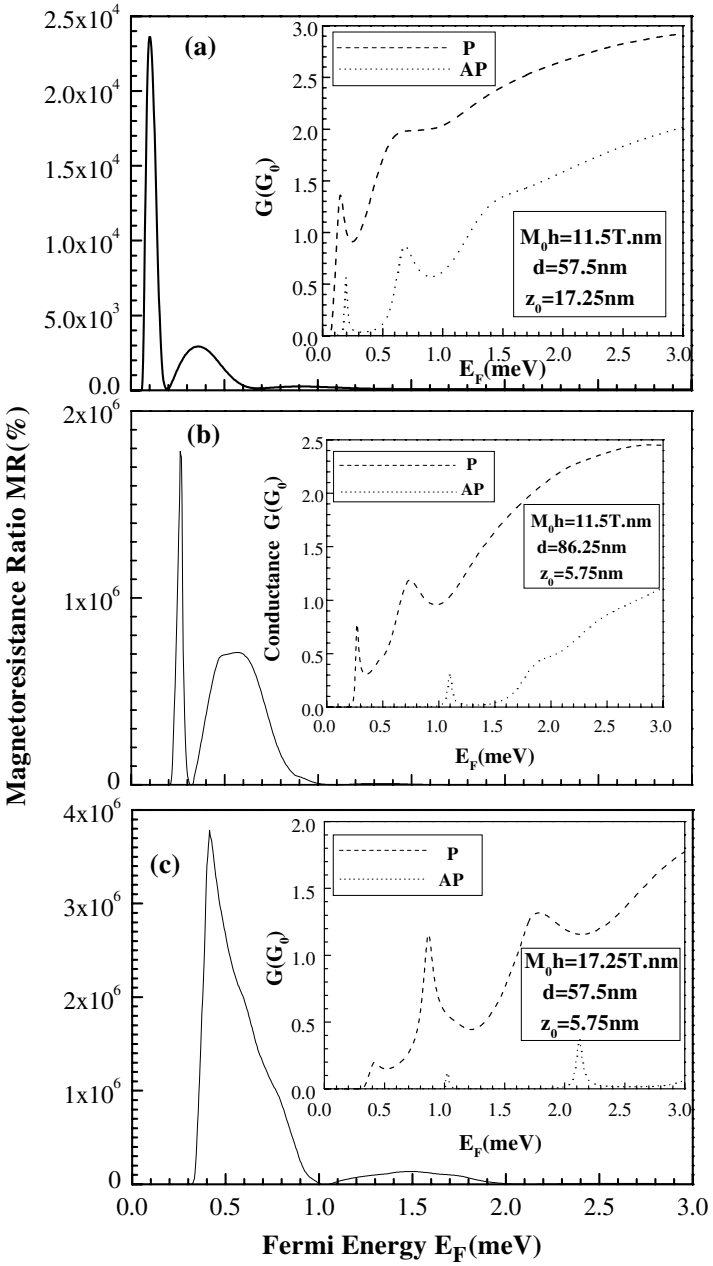

Figure 4. The magnetoresistance ratio MR versus the Fermi energy E_F for the device parameters (a) $M_0h = 11.5$ T nm, $d = 57.5$ nm, $z_0 = 17.25$ nm, (b) $M_0h = 11.5$ T nm, $d = 86.25$ nm, $z_0 = 5.75$ nm, and (c) $M_0h = 17.25$ T nm, $d = 57.5$ nm, $z_0 = 5.75$ nm respectively. The insets show their corresponding conductances G_A (dashed curve) and G_{AP} (dotted curve) and these conductances are also presented in G_0 for comparison.

ferromagnetic strips (increasing the parameter d) the conductance curves to the right and the difference between G_P and G_{AP} is increased. Therefore, the MR also shifts towards the high Fermi energy direction and increases greatly when ferromagnetic strips of the system become

wide. Figure 4(c) gives the results when the system parameters are $M_0h = 17.25$ T nm, $d = 57.5$ nm and $z_0 = 5.75$ nm. Comparing with figure 3, we can see from this plot that when M_0h increases, the conductance curves are suppressed, become much sharper and the discrepancy in conductances for the P and AP alignments is enhanced. We can also see that the MR curve shifts towards a much higher Fermi energy region, its peaks are widened and the MR ratio increases so that it is two orders of magnitude larger than that in figure 3. These effects of the ferromagnetic strips on the MR of the device are attributed to the variation of the effective potential of nanostructures because the parameters of the strips greatly influence the magnetic profiles (see the equation (1)). At the same time, these features also imply that one can greatly enlarge the magnetoresistance ratio (MR) of the device by means of proper fabrication of the ferromagnetic strips in the system.

4. Conclusions

In summary, we have constructed a GMR-like or LMR device based on the combination of non-homogeneous magnetic fields and a 2DEG, which can be experimentally realized by the deposition of two parallel metallic ferromagnetic strips on the top of a semiconductor heterostructure. We have theoretically investigated the LMR effect for electrons tunnelling through this system. Our calculations show that, since there exists an evident tunnelling difference in the P and AP configurations (especially the suppression of transmission for the AP alignment), this nanostructure shows a considerable GMR-like effect, which is strongly dependent upon the Fermi energy of electrons. We have also exhibited that the MR ratio is greatly influenced by the ferromagnetic strips and their distance to the 2DEG. Therefore, a much larger MR ratio can be achieved by properly fabricating the strips and by adjusting their locations relative to the 2DEG.

Acknowledgments

This work was supported by the National Major Project of Fundamental Research, Ministry of Sciences and Technology of China under grant no 1999064501, and by the National Natural Science Foundation of China under grant no 10074064.

References

[1] Baibich M N, Broto J M, Fert A, Nguyen Van Dau F, Petroff F, Etienne P, Creuzet G, Friederich A and Chazelas J 1988 *Phys. Rev. Lett.* **61** 2472
[2] Prinz G A 1998 *Science* **282** 1660
Wolf S A, Awschalom D D, Buhrman R A, Daughton J M, von Molnar S, Roukes M L, Chtchelkanova A Y and Treger D M 2001 *Science* **294** 1488
[3] Ross C A 2001 *Annu. Rev. Mater. Sci.* **31** 203
[4] Daughton J M, Pohm A V, Fayfield R T and Smith C H 1999 *J. Phys. D: Appl. Phys.* **32** R169
Daughton J M 1999 *J. Magn. Magn. Mater.* **192** 334
[5] Schad R, Potter C D, Belien P, Verbanck G, Moshchalkov V V and Bruynseraede Y 1994 *Appl. Phys. Lett.* **64** 3500
[6] Zhai F, Guo Y and Gu B L 2002 *Phys. Rev.* B **66** 125305
[7] Kubrak V, Rahnman F, Gallagher B L, Main P C, Henini M, Marrows C H and Howson M A 1999 *Appl. Phys. Lett.* **74** 2507
[8] Vancura T, Ihn T, Broderick S, Ensslin K, Wegscheider W and Bichler M 2000 *Phys. Rev.* B **62** 5074
[9] Matulis A, Peeters F M and Vasilopoulos P 1994 *Phys. Rev. Lett.* **72** 1518
[10] You J Q, Lide Zhang and Ghosh P K 1995 *Phys. Rev.* B **52** 17243
[11] Lu M W, Zhang L D, Jin Y X and Yan X H 2002 *Eur. Phys. J.* B **27** 565

Lu M W and Zhang L D 2002 *Semicond. Sci. Technol.* **17** 1184
[12] Levy P M 1994 *Solid State Phys.* **47** 367
Gijs M A M and Bauer G E W 1997 *Adv. Phys.* **46** 285
AnSermet J-Ph 1998 *J. Phys.: Condens. Matter* **10** 6027
[13] Schep K M, Kelly P J and Bauer G E W 1998 *Phys. Rev.* B **57** 8907
[14] Ferreira M S, d'Albuquerque e Castro J, Muniz R B and Villeret M 1999 *Appl. Phys. Lett.* **75** 2307
[15] Castano F J, Haratani S, Hao Y, Ross C A and Smith H 2002 *Appl. Phys. Lett.* **81** 2809
[16] Milano J, Llois A M and Steren L B 2002 *Phys. Rev.* B **66** 134405